Creep and fracture of a protein gel under stress: supplemental material

M. Leocmach,[1,*] C. Perge,[1] T. Divoux,[2] and S. Manneville[1]

[1] *Université de Lyon, Laboratoire de Physique, École Normale Supérieure de Lyon, CNRS UMR 5672, 46 Allée d'Italie, 69364 Lyon cedex 07, France*

[2] *Centre de Recherche Paul Pascal, CNRS UPR 8641 - 115 avenue Schweitzer, 33600 Pessac, France*

(Dated: June 12, 2014)

Supplemental movies

Supplemental Movie 1 shows the failure of a 4% wt. casein gel acidified with 4% wt. GDL in a plate-plate geometry for an imposed shear stress $\sigma = 120$ Pa. The plate diameter is 50 mm and the gap width is 1 mm. Fractures grow parallel to the vorticity direction, i.e. along the radial direction in this case. The global rheological response is fully similar to that measured in the Taylor-Couette (TC) geometry.

Supplemental Movie 2 shows the creep experiment analyzed in Figs. 3 and 4 and performed under $\sigma = 300$ Pa on a 4% wt. casein gel seeded with 3% wt. polyamide spheres and acidified with 1% wt. GDL. The gap width of the TC cell is 2 mm and its height is 60 mm. Images recorded by a standard webcam (Logitech Webcam Pro 9000) are shown in the top left panel. Velocity maps $v(r, z, t)$ inferred from ultrasonic imaging by averaging over 4 s are shown in the top right panel using linear color levels. The vertical position $z = 0$ on the ultrasonic images corresponds to about 15 mm below the top of the TC cell. The two bottom graphs show the global shear rate response $\dot{\gamma}(t)$ (left) and the strain response $\gamma(t)$ recorded by the rheometer (AR G2, TA Instruments) simultaneously to optical and ultrasonic imaging.

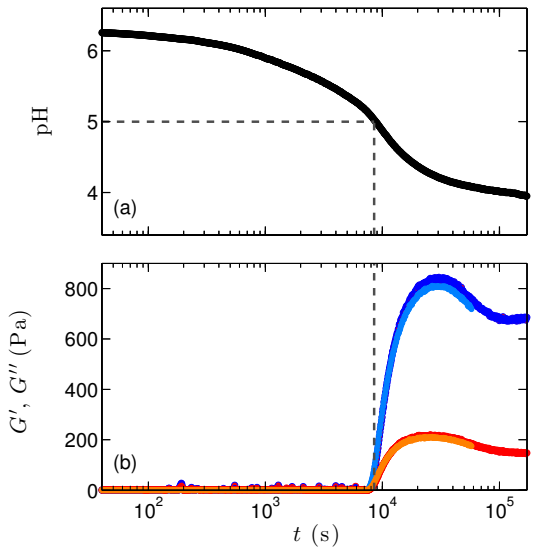

FIG. 1: (color online) Gelation process of a 4% wt. casein suspension seeded with 3% wt. polyamide spheres and acidified with 1% wt. GDL. (a) pH vs time t. (b) Linear viscoelastic moduli G' (top, in blue) and G'' (bottom, in red) recorded as a function of time t for fixed frequency $f = 1$ Hz and strain amplitude 0.1%. Dashed lines indicate that the system starts to build significant elastic properties when the pH decreases below about 5. Lighter colors in (b) correspond to a sample free of polyamide spheres, showing that the addition of acoustic contrast agents does not affect significantly the gelation process and the final viscoelastic properties of the gel.

Supplemental figures

Supplemental Figure 1 illustrates the gelation process of a 4% wt. sodium caseinate solution seeded with 3% wt. polyamide spheres through time-resolved measurements of the elastic and viscous moduli, respectively G' and G'', under small amplitude oscillatory shear. GDL contains an ester function which, once added to the solution at time $t = 0$, hydrolyzes spontaneously and leads to a slow decrease of the pH [Suppl. Fig. 1(a)] towards the casein isoelectric point (pH $\simeq 4.6$) at which casein particles aggregate. Gelation actually starts earlier at pH $\simeq 5$ as shown by gray dashed lines and as already discussed in Ref. [1]. At this point the elastic and viscous moduli display a sudden increase then overshoot and converge towards their steady-state values where $G' \gg G''$ [Suppl. Fig. 1(b)]. Note that the maximum of the overshoot is

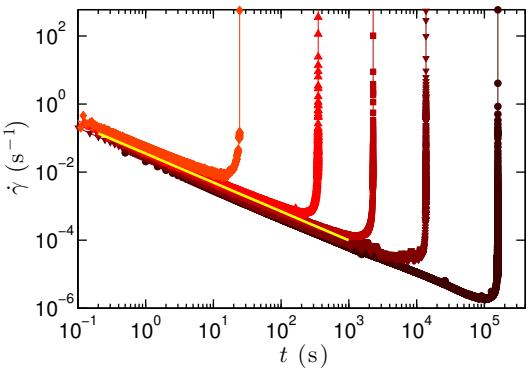

FIG. 2: (color online) Shear rate response $\dot{\gamma}(t)$ in a 4% wt. casein gel acidified with 1% wt. GDL for an imposed shear stress $\sigma = 200$ (●), 300 (▼), 400 (■), 550 (▲) and 1000 Pa (♦) from right to left. The gap width is 1 mm. The yellow line shows the power-law behavior $\dot{\gamma}(t) \sim t^{-0.85}$.

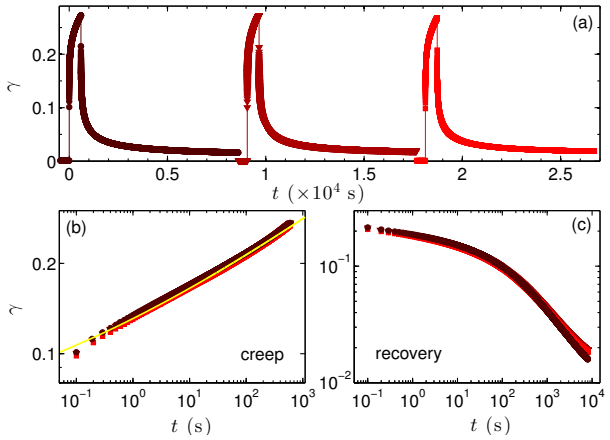

FIG. 3: (color online) Three creep and recovery tests preformed successively in the primary creep regime on the same 4% wt. casein gel acidified with 1% wt. GDL. Prior to each test, the viscoelastic moduli are measured over 450 s under small amplitude oscillations around the reference position $\gamma = 0$ (see Suppl. Fig. 4). A constant stress $\sigma = 100$ Pa is then applied for 600 s and finally the relaxation at $\sigma = 0$ is followed over 8,000 s. (a) Full strain response $\gamma(t)$ vs time. (b) Superimposed strain responses during the three successive creep tests at $\sigma = 100$ Pa and plotted in logarithmic scales as a function of the time since stress application. The yellow line is $\gamma(t) = 0.048 + 0.083 t^{0.15}$. (c) Superimposed strain responses during the three recovery phases and plotted in logarithmic scales as a function of the time since stress is removed.

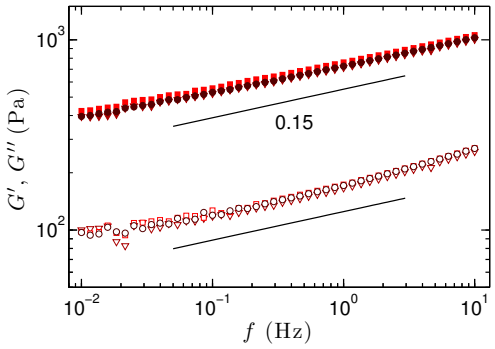

FIG. 4: (color online) Linear viscoelastic moduli G' (top) and G'' (bottom) as a function of frequency f for a strain amplitude of 0.1% recorded before each creep and recovery test shown in Suppl. Fig. 3. The symbols ●, ▼ and ■ respectively correspond to the first, second and third tests. Black lines are power laws $G' \sim G'' \sim f^{0.15}$.

reached around the isoelectric point. The decrease of both moduli at lower pH is usually attributed to the over-acidification which enhances the repulsive electrostatic interactions between casein particles of net positive charge [2].

Supplemental Figure 2 shows the shear rate $\dot{\gamma}(t)$ obtained by differentiating the raw strain of Fig. 1 in the main text. For $0.1 \lesssim t/\tau_f \lesssim 0.9$, i.e. in the secondary creep regime, $\dot{\gamma}(t)$ is smoothed using a moving average over $\delta t \simeq 0.01\tau_f$ in order to remove high-frequency noise due to differentiation at very small shear rates. For the largest applied shear stress $\sigma = 1000$ Pa at times $t < 0.1$ s, oscillations are observed in $\gamma(t)$ and consequently in $\dot{\gamma}(t)$ (negative values of the shear rate do not show in Suppl. Fig. 2 due to logarithmic scales). These short-time oscillations, which are well documented in the rheology literature [3], arise from the coupling between the sample viscoelasticity and the instrument inertia. Here they impose an experimental limit to the extension of the power-law scaling $\dot{\gamma}(t) \sim t^{-0.85}$ at short times. The shear rate data normalized by its minimum value $\dot{\gamma}_{\min}$ is plotted in Fig. 2(a) as a function of t/τ_f once all oscillations have died out. This leads to a nice collapse onto a single curve whatever the imposed shear stress.

Successive creep and recovery experiments performed on the same sample within the primary creep regime are presented in Supplemental Figures 3 and 4. When a stress of 100 Pa is applied at time $t = 0$, an "instantaneous" elastic strain of about 10% is recorded, followed by the slow Andrade-like creep already investigated in the main text and characterized by an exponent of 0.15 [Suppl. Fig. 3(b)] that coincides with that of the frequency-dependence of both viscoelastic moduli G' and G'' [Suppl. Fig. 4]. When stress is removed at $t = 600$ s, the strain drops by about 6% and then slowly relaxes over several hours. After 8,000 s we observe that the initial strain is almost fully recovered: only a few percents are not (here 2% out of a total maximum strain of 27%).

Such an irrecoverable strain can be attributed either to viscous flow within the porous structure of the gel or to plastic events i.e. to local rupture of the gel network, and in the most general case to a combination of both. Interestingly, when the strain is reset to zero between two successive creep and recovery tests [i.e. the moving tool is moved back to its initial position, see the corresponding trace in Suppl. Fig. 3(a)], the strain responses are indistinguishable [Suppl. Fig. 3(b) and (c)]. If significant plastic deformation had occurred during the first loading–unloading cycle, one would have expected the second and third responses to the same cycle to differ significantly, e.g. through larger maximum strains or larger unrecoverable strains.

Finally Supplemental Figure 4 shows that both viscoelastic moduli G' and G'' do not change significantly from one creep and recovery test to another and that their scaling with the frequency remains the same. This indicates that the gel microstructure is mostly undamaged by creep within the primary regime.

* Electronic address: mathieu.leocmach@ens-lyon.fr

[1] J.A. Lucey and H. Singh, Food Res. Int. A **30**, 529–542

(1998).
[2] E. Dickinson and L.M. Merino, Food Hydrocolloid **16**, 321–331 (2002).
[3] G. Benmouffok-Benbelkacem et al., Rheol Acta **49**, 305–314 (2010).